Proceedings of the European Conference Physics of Magnetism, Poznań 2017

Effect of Nd^{3+} Doping on Magnetic and Dielectric Properties of $SrFe_{12}O_{19}$ Hexaferrite Synthesized by Coprecipitation Method

A. Hilczer[a,*], K. Pasińska[b], E. Markiewicz[a], A. Pietraszko[b], B. Andrzejewski[a]
[a]Institute of Molecular Physics, Polish Academy of Sciences, M. Smoluchowskiego 17, 60-179 Poznań, Poland
[b]Institute of Low Temperature and Structure Research, Polish Academy of Sciences, Okólna 2, 50-422 Wrocław, Poland

Magnetic and dielectric properties of hexagonal ferrites important for applications in microwave absorbers are strongly determined by the processing conditions. We studied dielectric and magnetic response of $Sr_{1-x}Nd_xFe_{12}O_{19}$ (x = 0, 0.03, 0.05, 0.07, 0.09) solid solutions obtained by coprecipitation method. The structure of the samples was controlled by X-ray diffraction and scanning electron microscope images revealed that the powder is a mixture of small nanograins and crystallites of 500 nm–1 μm in size. Nd^{3+} doping was found to result in an increase in the coercive field which we would like to relate to the domain wall pinning. The doping-induced changes are monotonous with x up to 0.07. The observed dispersion of permittivity was found to be correlated with the frequency behaviour of electric conductivity of the samples.

DOI: 10.12693/APhysPolA.133.669
PACS/topics: 75.50.Gg, 75.60.Ej, 75.75.+a, 81.20.Fw

1. Introduction

M-type hexagonal ferrites with large magnetocrystalline anisotropy and high electric resistivity are essential for various applications, among others in high frequency devices [1–3]. Rare earth (RE) substitution $A_{1-x}(RE)_xFe_{12}O_{19}$ (A = Ba, Sr, Pb) has been used to control the spin-orbit interaction and to modify the magnetic properties [4–9]. Solubility of the RE ions was however, found to be limited to $x \leqslant 0.1$ due to the shape of electronic charge distribution and its surrounding in the crystal [5]. M-type hexaferrites crystallize in hexagonal structure with $P6_3/mmc$ space group (No 194) and $Z = 2$. Their magnetic properties are determined by 24 Fe^{3+} ions distributed in the lattice in sites of tetrahedral symmetry ($4f_1$ Wyckoff positions), of octahedral symmetry ($Z = 2$, $2a$, $4f_2$) and in bipyramidal sites ($2b$) [3]. According to the Gorther model magnetic moment of the unit cell amounts to 40 μ_B and results from the superposition of magnetic moments (5 μ_B) of 16 Fe^{3+} ions parallel to the hexagonal axis ($Z = 2$, $2b$, $2a$) and 8 moments of ($4f_1$, $4f_2$) Fe^{3+} aligned antiparallel to the c-axis [10]. Nanosized materials are very promising to increase the performance of various devices however, their magnetic properties are highly sensitive to microstructure (size and shape) of the nanoparticles [11, 12]. As only few papers [4, 8, 9] are devoted to the effect of Nd^{3+} doping on magnetic properties of SrM hexaferrite nanoparticles we proceeded to study magnetic and dielectric behavior of $Sr_{1-x}Nd_xFe_{12}O_{19}$ nanopowder obtained by chemical coprecipitation.

*corresponding author; e-mail: ahilczer@ifmpan.poznan.pl

2. Experimental

$Sr_{1-x}Nd_xFe_{12}O_{19}$ with x = 0, 0.03, 0.05, 0.07 and 0.09 were prepared by coprecipitation method from following precursors: $Sr(NO_3)_2$, $Fe(NO_3)_3 \cdot 9H_2O$, HNO_3, Nd_2O_3, NH_3, and $H_2C_2O_4 \cdot 2H_2O$. 20% NH_4OH was added to achieve pH = 7 and precipitate the metal solution. The precipitate was washed several times with deionized water and dried powders were sintered for 24 h at 400 °C and calcined at 1200 °C for 4 h in the air.

The structure of the samples was controlled by X-ray diffraction (X'Pert PANalytical, CuK_α) in Bragg-Brentano geometry and refined by Rietveld method using a High Score Plus package. The morphology was studied by scanning electron microscopy FEI Nova NanoSEM with incident electron energy of 5 keV.

Physical Property Measurement System (PPMS, Quantum Design Ltd) with vibrating sample magnetometer probe was used for magnetic measurements in the temperature range 4–300 K. Dielectric response and ac conductivity of the samples (powder pressed at 0.6 GPa into pellets with Au-evaporated electrodes) were studied using an Alpha-A High Performance Frequency Analyzer (Novocontrol GmbH) in the frequency range 10 mHz–1 MHz and up to 1 GHz using an E4991A RF Impedance/Material Analyzer Agilent.

3. Results and discussion

As shown in Fig.1 the Nd-doped SrM samples contain a single phase only, whereas a trace of α-Fe_2O_3 parasite (marked by arrows) is apparent in the undoped $SrFe_{12}O_{19}$ sample. Nd^{3+} with ionic radius R_{Nd} = 98 pm < R_{Sr} = 118 pm [13] induces also a small but continuous decrease in the lattice parameters. The decrease in a and c amounts to 0.2% and 0.5%, respectively

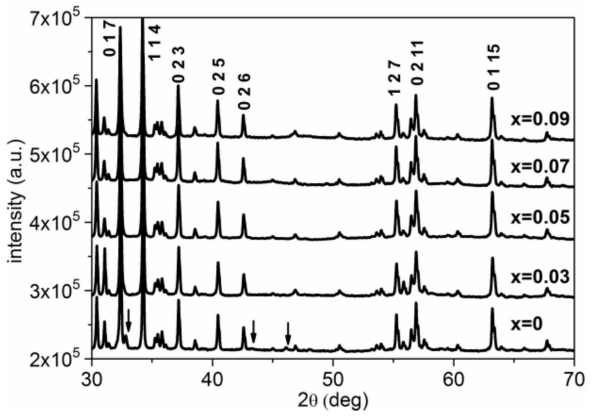

Fig. 1. Room temperature XRD pattern of $Sr_{1-x}Nd_xFe_{12}O_{19}$.

for sample with $x = 0.09$ which is in an agreement with the literature data [5].

SEM images (not shown here) have revealed that the $Sr_{1-x}Nd_xFe_{12}O_{19}$ powders are a mixture of small grains (of average size 50–100 nm) and crystallites with mean sizes from $\sim$ 500 nm to $\sim$ 1 μm. The mean size of the crystallites decreases sligthly with Nd doping but the powder remains still bimodal.

Magnetic properties of hexaferrites are related to the ferric ions which coupled with O^{-2} form a colinear magnetic order. Figure 2 shows examples of hysteresis loop, which are characteristic of ferro/ferrimagnetic order. Detailed studies show that the loops of Nd-doped samples exhibit curling modes (see the inset) due to an incoherent magnetization reversal [11, 12] in the crystallites with sizes greater than the crictical particle size d_{cr} of a single domain state ($d_{cr} \approx 650$ nm for SrM [14]).

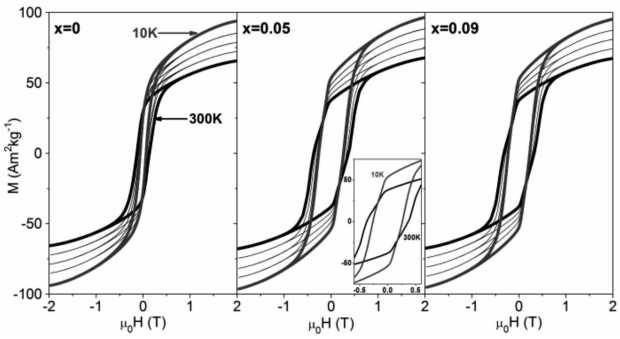

Fig. 2. Magnetic hysteresis loops of $Sr_{1-x}Nd_xFe_{12}O_{19}$ at 10, 150, 200, 250, and 300 K; $dH/dt = 50$ Oe/s.

One can observe that the coercive field of $Sr_{1-x}Nd_xFe_{12}O_{19}$ increases monotoneously with the concentration of the dopant up to $x = 0.07$ (Fig. 3). The effect we would like to relate to the domain wall pinning. The admixture of Nd^{3+} ions (exhibiting magnetic moment of 3.5 μ_B) results also in a small improvement the effective magnetic moment: the magnetization value $M_{2\ T}$ in field of 2 T increases by $\sim$ 3–4% at 300 K. Figure 4 shows temperature variation in the H_c and $M_{2\ T}$ for pure and Nd-doped SrM hexaferrites. The coercivity of doped samples is found to increase with rising temperature, similarly to the behaviour observed for pure M-type pure hexaferrites. The decrease in the magnetization value $M_{2\ T}$ at higher temperatures is due the Bloch law $M \sim T^{3/2}$.

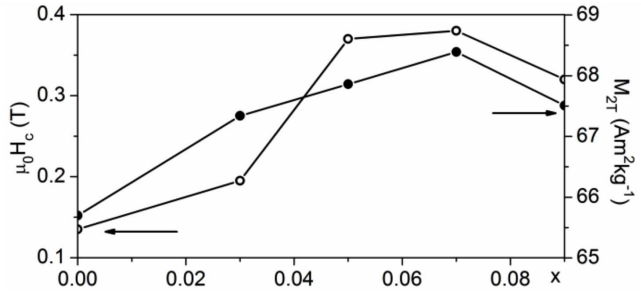

Fig. 3. Room temperature coercivity H_c and magnetization $M_{2\ T}$ of $Sr_{1-x}Nd_xFe_{12}O_{19}$ *versus* x.

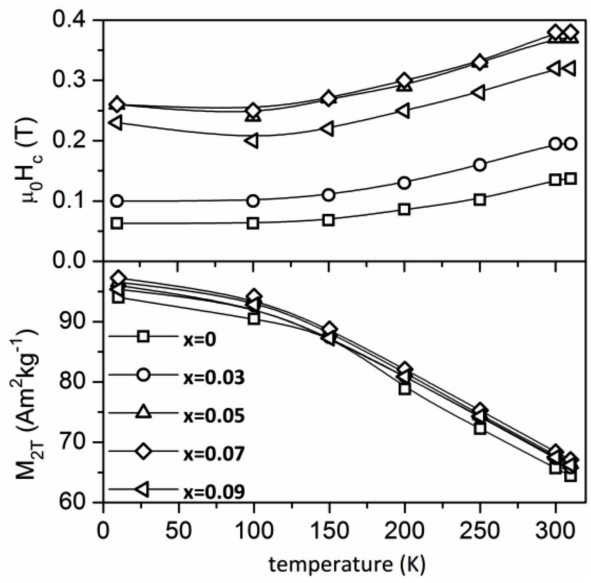

Fig. 4. Temperature variation of coercive field H_c and magnetization $M_{2\ T}$ for $Sr_{1-x}Nd_xFe_{12}O_{19}$.

Correlation between frequency behavior of electric conductivity and permittivity of the ferrites has been related by Koops to the heterogeneity of the ceramics consisting of highly conducting grains separated by grain boundaries with high electric resistivity [15]. Iwauchi has shown that electron hopping between ferric and ferrous ions $Fe^{3+} + e^- \rightarrow Fe^{2+}$ is responsible for the conductivity [16]. In the case of M-type hexaferrites electron hopping between Fe4–Fe4 ($4f_2$) and Fe5–Fe5 ($Z = 2$) ions in the octahedral sites was reported to be responsible for electric transport [17]. Figure 5 shows examples of frequency

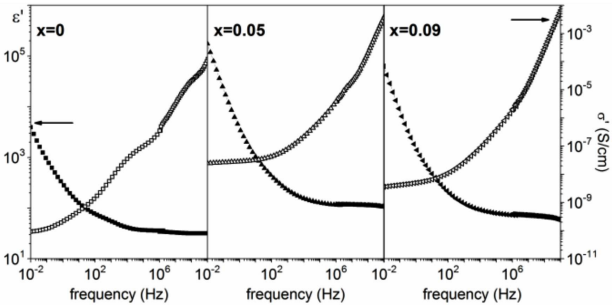

Fig. 5. Frequency dependence of permittivity ε' and electric conductivity σ' of $Sr_{1-x}Nd_xFe_{12}O_{19}$ at room temperature.

dependences of permittivity and electric conductivity of $Sr_{1-x}Nd_xFe_{12}O_{19}$.

One can observe that for $x \geqslant 0.05$ the permittivity ε' decreases rapidly at low frequencies and reaches a constant value at $f_a \approx 10$ kHz, whereas at this frequency the conductivity starts to increase (being below f_a rather low and frequency independent). Thus the low-frequency behavior of ε' is determined by space charge polarization piled up at poorly conducting grain boundaries and the contribution from insulator-electrode contact [18]. With increasing frequency of externally applied electric field electrons hopping between the localized ferric and ferrous cations cannot follow the alternating field and the permittivity decreases reaching a constant value. The high frequency permittivity value can be considered as characteristic of the grain interior of our hexaferrite ceramics.

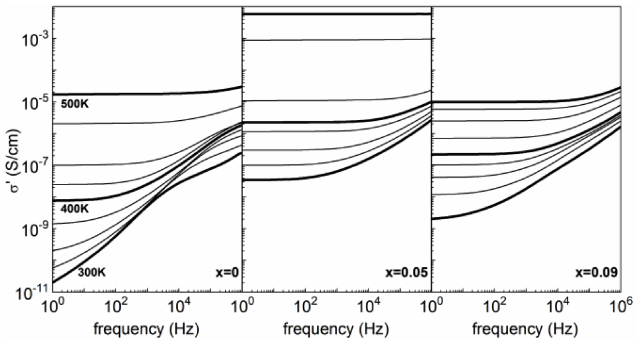

Fig. 6. Electric conductivity of $Sr_{1-x}Nd_xFe_{12}O_{19}$ *versus* frequency measured at constant temperature in the range from 300 K to 500 K with a step of 25 K.

The effect of thermal activation of electron hopping, apparent in frequency dependences of electric conductivity at higher temperatures is shown in Fig. 6. One can observe that the space charge polarization persists also at high frequencies. Nd-doping was found to increase the conductivity of the hexaferrites and Fig. 7 shows the dc conductivity at 300 and 500 K as dependent on the concentration of the dopant.

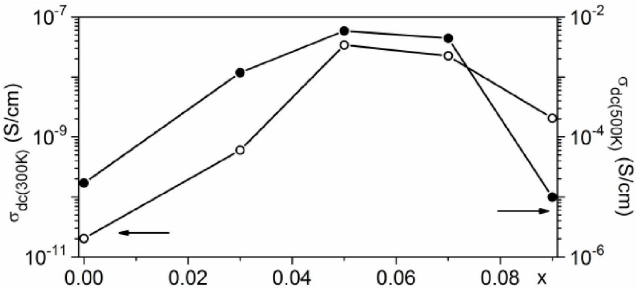

Fig. 7. dc electric conductivities of $Sr_{1-x}Nd_xFe_{12}O_{19}$ at 300 K and at 500 K as dependent on the concentration $x$of Nd^{3+} ions.

4. Conclusions

$Sr_{1-x}Nd_xFe_{12}O_{19}$ with $0 \leqslant x \leqslant 0.09$ obtained by precipitation method is a single phase compound and can be considered as consisting of a mixture of single magnetic domain grains and multidomain crystallites. The bimodal morphology is apparent in the hysteresis loop as curling modes and the doping-induced increase in the coercivity is related to the domain wall pinning effect. Nd^{3+} ions substituting divalent Sr^{2+} ions in the hexaferrite lattice with magnetic moment of 3.5 μ_B result also in an increase of the electric conductivity and space charge polarization due to formation additional oxygen vacancies and moreover, are responsible for the small increase of the effective magnetic moment. The modification of magnetic and dielectric properties induced by Nd^{3+} doping of $SrFe_{12}O_{19}$ hexagonal ferrite reaches maximum for the doping level of 0.05-0.07%.

References

[1] V.G. Harris, A. Geiler, Y. Chen, S.D. Yoon, M. Wu, A. Yang, Z. Chen, P. He, P.V. Parimi, X. Zuo, C.E. Patton, M. Abe, O. Acher, C. Vittoria, *J. Magn. Magn. Mater.* **321**, 2035 (2009).

[2] V.G. Harris, *IEEE Trans. Magn.* **48**, 1075 (2012).

[3] R.C. Pullar, *Progress Mater. Sci.* **57**, 1191 (2012).

[4] J.F. Wang, C.B. Ponton, I.R. Harris, *IEEE Trans. Magn.* **48**, 1075 (2002).

[5] L. Lechevallier, J.M. Le Breton, A. Morel, P. Tenaud, *J. Phys.: Condens. Matter* **20**, 1715203 (2008).

[6] A. Singh, S.B. Narang, K. Singh, O.P. Pandey, R.K. Kotnala, *J. Ceram. Process. Res.* **11**, 241 (2010).

[7] T.J. Pérez-Juache, I. Betancourt, S.A. Palomares-Sánchez, M. Mirabal García, J.A, Matutes-Aquino, A.L. Guerrero-Serrano, *J. Supercond. Nov. Magn.* **24**, 2325 (2011).

[8] J. Luo, *Mater. Lett.* **80**, 162 (2012).

[9] A. Thakur, R.R. Singh, P.B. Barman, *Mater. Chem. Phys.* **141**, 562 (2013).

[10] E.W. Gorter, *Proc. IEE Part B* **104**, 255 (1957).

[11] R. Skomski, *J. Phys.: Condens. Matter* **15**, R841 (2003).

[12] A. Enders, R. Skomski, J. Honolka, *J. Phys.: Condens. Matter* **22**, 433001 (2010).

[13] R.D. Shannon, *Acta Cryst. A* **32**, 751 (1976).

[14] Z.F. Zi, Y.P. Sun, X.B. Zhu, Z.R. Yang, J.M. Dai, W.H. Song, *J. Magn. Magn. Mater.* **320**, 2746 (2008).

[15] C.G. Koops, *Phys. Rev.* **83**, 121 (1951).

[16] K. Iwauchi, *Jpn. J. Appl. Phys.* **10**, 1520 (1971).

[17] K. Kimura, M. Ohgaki, K. Tanaka, H. Morikawa, F. Marumo, *J. Solid State Chem.* **87**, 186 (1990).

[18] P. Lunkenheimer, V. Bobnar, A.V. Pronin, A.I. Ritus, A.A. Volkov, A. Loidl, *Phys. Rev. B* **66**, 052105 (2002).